

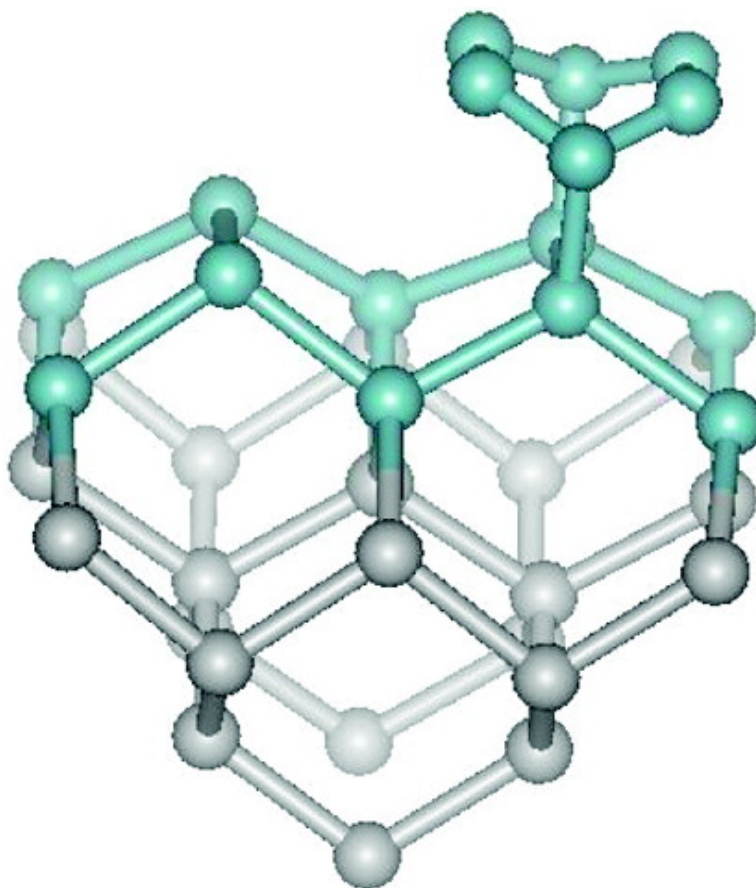
Article

## Cycloaddition of Benzene on Si(100) and Its Surface Conversions

Yousung Jung, and Mark S. Gordon

*J. Am. Chem. Soc.*, **2005**, 127 (9), 3131-3139 • DOI: 10.1021/ja0402093 • Publication Date (Web): 10 February 2005

Downloaded from <http://pubs.acs.org> on March 24, 2009



### More About This Article

Additional resources and features associated with this article are available within the HTML version:

- Supporting Information
- Links to the 10 articles that cite this article, as of the time of this article download
- Access to high resolution figures



**ACS Publications**  
High quality. High impact.

- Links to articles and content related to this article
- Copyright permission to reproduce figures and/or text from this article

[View the Full Text HTML](#)



## Cycloaddition of Benzene on Si(100) and Its Surface Conversions

Yousung Jung<sup>†</sup> and Mark S. Gordon\*

Contribution from the Department of Chemistry, Iowa State University, Ames, Iowa 50011

Received September 7, 2004; E-mail: mark@si.fi.ameslab.gov

**Abstract:** A comprehensive ab initio study of the adsorption of benzene on the silicon(100) surface is presented. Five potential candidates ([2+2] adduct, [4+2] adduct, two tetra- $\sigma$ -bonded structures, and one radical-like structure) for the reaction product are examined to determine the lowest energy adsorption configuration. A [4+2] butterfly structure is determined to be the global minimum (−29.0 kcal/mol), although one of the two tetra- $\sigma$ -bonded structures (−26.7 kcal/mol) is similar in energy to it. Multireference perturbation theory suggests that the [4+2] addition mechanism of benzene on Si(100) is very similar to the usual Diels–Alder reaction (i.e., small or zero activation barrier), even though benzene adsorption entails the loss of benzene aromaticity during the reaction. On the other hand, the [2+2] cycloaddition mechanism is shown to require a relatively high activation barrier (17.8 kcal/mol), in which the initial step is to form a (relatively strongly bound) van der Waals complex (−8.9 kcal/mol). However, the net activation barrier relative to reactants is only 8.9 kcal/mol. Careful examination of the interconversion reactions among the reaction products indicates that the two tetra- $\sigma$ -bonded structures (that are energetically comparable to the [4+2] product) can be derived from the [2+2] adduct with activation barriers of 15.5 and 21.4 kcal/mol. However, unlike the previous theoretical predictions, it is found that the conversion of the [4+2] product to the tetra- $\sigma$ -bonded structures entails huge barriers (>37.0 kcal/mol) and is unlikely to occur. This suggests that the [4+2] product is not only thermodynamically the most stable configuration (lowest energy product) but also kinetically very stable (large barriers with respect to the isomerization to other products).

### I. Introduction

Organic modification of semiconductor surfaces is becoming very popular due to its industrial importance for the development of new functional surfaces and molecular-scale electronics. Such surfaces, modified with organic molecules, can attain additional useful properties such as optical activity and biofunctionality. For example, Lopinski et al. recently showed that a chiral surface can be prepared by introducing (1*S*)-(+)-3-carene onto the silicon(100) surface.<sup>1</sup>

In addition, introducing hydrocarbons onto the Si(100) surface is a potentially important process for SiC film growth. Studies on ethylene and acetylene on Si(100) have shown that C–C  $\pi$  bonds in alkenes or alkynes can readily react with the dangling bonds of the surface dimer of the reconstructed Si(100) surface.<sup>2–9</sup> The carbons in these unsaturated hydrocarbons undergo rehybridization to form Si–C  $\sigma$  bonds with the silicon surface dimers. The adsorption product is thereby similar to the [2+2] four-membered-ring cycloaddition adduct. While the

adsorption of many unsaturated hydrocarbons on Si(100) is essentially irreversible, previous thermal desorption experiments showed that benzene adsorbs and desorbs almost reversibly on the Si(100) surface.<sup>10</sup>

Taguchi and co-workers used TDS, EELS, LEED, and AES spectroscopic tools and demonstrated that benzene is chemisorbed nondissociatively onto the silicon surface at both 90 and 300 K.<sup>10</sup> Chemisorbed benzene was observed to have both sp<sup>2</sup>- and sp<sup>3</sup>-hybridized carbon atoms. They estimated the fractional saturation coverage of benzene on Si(100) to be ~0.27 ML, which corresponds to one benzene molecule per two surface silicon dimers (1 ML means one target molecule per surface atom). On the basis of their experimental data, they proposed two possible candidates for the adsorption product, **1** and **2** in Chart 1. Structures **1** and **2** correspond to [2+2] and [4+2] cycloaddition products, respectively.

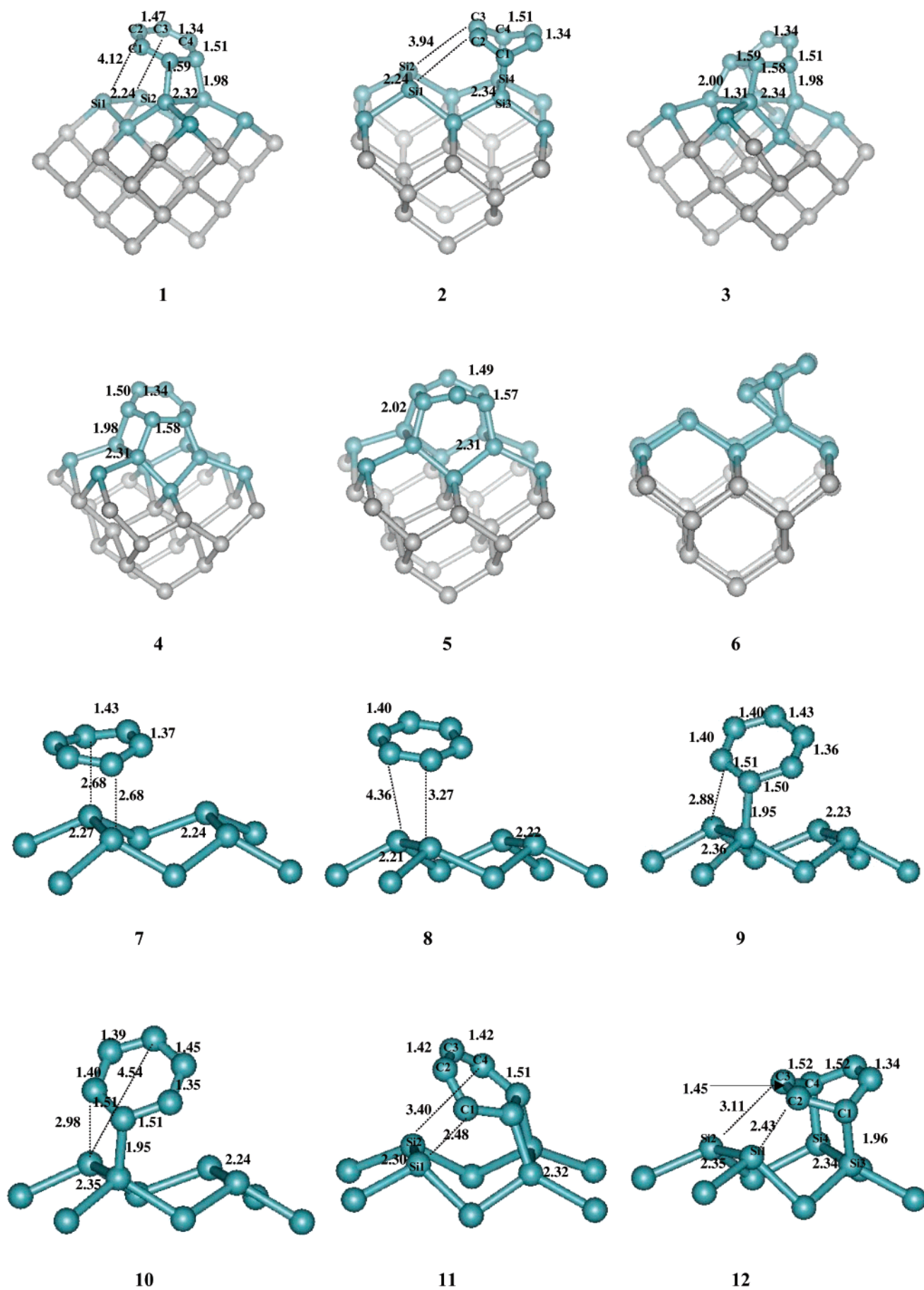
Theoretical results for the adsorption structures of benzene on Si(100) were first presented by Craig using the SLAB-MINDO semiempirical method.<sup>11</sup> A number of possible product configurations were compared, and [2+2]-like products (**1** and

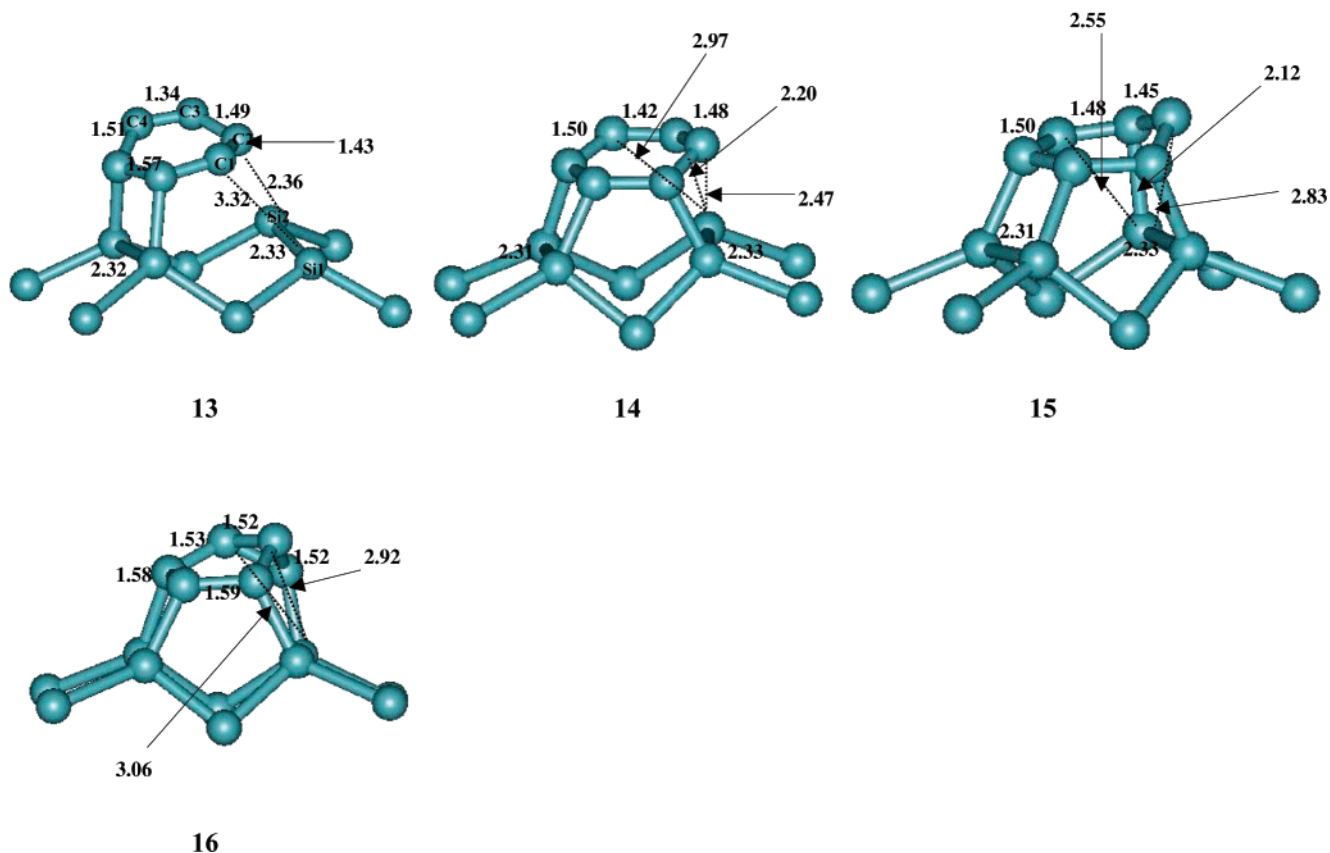
<sup>†</sup> Current address: Department of Chemistry, University of California, Berkeley, CA 94720.

(1) Lopinski, G. P.; Moffatt, D. J.; Wayner, D. D. M.; Wolkow, R. A. *J. Am. Chem. Soc.* **2000**, *122*, 3548.  
(2) Yoshinobu, J.; Tsuda, H.; Onchi, M.; Nishijima, M. *J. Chem. Phys.* **1987**, *87*, 7332.  
(3) Widdra, W.; Huang, C.; Weinberg, W. H. *Surf. Sci.* **1995**, *329*, 295.  
(4) Widdra, W.; Huang, C.; Yi, S. I.; Weinberg, W. H. *J. Chem. Phys.* **1996**, *105*, 5605.  
(5) Nishijima, M.; Yoshinobu, J.; Tsuda, H.; Onchi, M. *Surf. Sci.* **1987**, *192*, 383.

(6) Imamura, Y.; Morikawa, Y.; Yamasaki, T.; Nakatsuji, H. *Surf. Sci.* **1995**, *341*, L1091.  
(7) Liu, Q.; Hoffmann, R. *J. Am. Chem. Soc.* **1995**, *117*, 4082.  
(8) Li, L.; Tindall, C.; Takaoka, O.; Hasegawa, Y.; Sakurai, T. *Phys. Rev. B* **1997**, *56*, 4648.  
(9) Wolkow, R. A. *Annu. Rev. Phys. Chem.* **1999**, *50*, 413.  
(10) Taguchi, Y.; Fujisawa, M.; Takaoka, T.; Okada, T.; Nishijima, M. *J. Chem. Phys.* **1991**, *95*, 6870.  
(11) Craig, B. I. *Surf. Sci.* **1993**, *280*, L279.

Chart 1





**6** in Chart 1) were suggested as preferred structures. Other semiempirical calculations by Jeong et al.<sup>12</sup> followed. The PM3 semiempirical method with a Si<sub>43</sub>H<sub>32</sub> four-layer cluster model was used, and a symmetric diradical-like structure, **5**, was predicted to be the most stable adsorption product. However, in those calculations, several geometric constraints were imposed on the surface structure. This could be particularly inappropriate because the surface dimer with partial double bond character will be rehybridized into a fully single bond during the surface reaction, and structural constraints on the surface dimer certainly cannot describe this phenomenon correctly.

A combined experimental and theoretical study of the adsorption of benzene on Si(100) was conducted by Gokhale et al.<sup>13,14</sup> Angle-resolved photoemission spectra suggested that the reaction product should have local  $C_{2v}$  symmetry with the molecular plane parallel to the surface dimer. On the basis of this local  $C_{2v}$  symmetry argument, two possible structures were predicted, the [4+2] and symmetric diradical-like structures (**2** and **5** in Chart 1). Their density functional theory (DFT) calculations with Si<sub>15</sub>H<sub>16</sub> and Si<sub>13</sub>H<sub>13</sub> cluster models further suggested that **2** is energetically the most stable product.

On the other hand, the STM experiments by Lopinski et al. suggested three different configurations for the reaction product:<sup>15–17</sup> one corresponding to a di- $\sigma$ -bonded geometry (**2**) on top of a single dimer, and two corresponding to a tetra- $\sigma$ -bonded geometry (**3** and **4**) arranged over two dimers. Their

STM images as a function of time also indicated that, while a single dimer state (di- $\sigma$ -bonded structure) was populated preferentially upon adsorption, it was converted to a tetra- $\sigma$ -bonded structure bridging two dimers on a longer time scale. This suggests that the single dimer geometry is metastable. The activation barrier for this conversion (from **2** to **3**) was estimated to be 0.95 eV (22 kcal/mol). Comparison of the real STM images with the simulated ones (by the calculation of charge density isosurfaces of occupied valence states) verified that **2** is the metastable single dimer state, and **3** and **4** are the two final bridge states. Their DFT/HF (Hartree–Fock) calculations (B3LYP/6-31G(d) single-point energy correction after geometry optimization with HF/3-21G(d)) further suggested that **3** (one of the bridge states) is the global minimum.

Interconversion between the adsorption products was also suggested by Borovsky et al. using STM experiments.<sup>18</sup> They found that the metastable species is symmetric, and that the final state to which the metastable species converts is located over two surface dimers. On the basis of these findings, they proposed that **2** is metastable and **1** is the final state. The activation barrier for this conversion was predicted to be about 23 kcal/mol, assuming a prefactor of  $10^{13}$  Hz. Although this conversion barrier is similar to the one previously suggested by Lopinski et al., it should be noted that the types of conversion are different: one is from **2** to **1** and the other is from **2** to **3** (or **4**).

Another experimental study using vibrational IR spectroscopy, thermal desorption, and near-edge X-ray absorption fine struc-

(12) Jeong, H. D.; Ryu, S.; Lee, Y. S.; Kim, S. *Surf. Sci.* **1995**, *344*, L1226.

(13) Birkenheuer, U.; Gutdeutsch, U.; Rosch, N. *Surf. Sci.* **1997**, *409*, 213.

(14) Gokhale, S.; Trischberger, P.; Menzel, D.; Widdra, W.; Droge, H.; Steinruck, H.-P.; Birkenheuer, U.; Gutdeutsch, U.; Rosch, N. *J. Chem. Phys.* **1998**, *108*, 5554.

(15) Lopinski, G. P.; Moffatt, D. J.; Wolkow, R. A. *Chem. Phys. Lett.* **1998**, *282*, 305.

(16) Lopinski, G. P.; Fortier, T. M.; Moffatt, D. J.; Wolkow, R. A. *J. Vac. Sci. Technol. A* **1998**, *16*, 1037.

(17) Wolkow, R. A.; Lopinski, G. P.; Moffatt, D. J. *Surf. Sci. Lett.* **1998**, *416*, L1107.

(18) Borovsky, B.; Krueger, M.; Ganz, E. *Phys. Rev. B* **1998**, *57*, R4269.



ture (NEXAFS) showed that benzene is predominantly physisorbed at cryogenic temperature (100 K) and chemisorbed at room temperature (300 K).<sup>19</sup> Structure **2** was suggested as an adsorption product by the authors, even though they also observed the presence of another structure, proposed to be a (less stable) tetra- $\sigma$ -bonded structure, namely **4** in Chart 1, on a time scale of hours.

The existence of metastable adsorption states was also suggested theoretically by Silvestrelli and co-workers.<sup>20</sup> In their study, they predicted tetra- $\sigma$ -bonded structures (**3** and **4** in Chart 1) to be the most stable configurations and three different “butterfly” structures (including **2** in Chart 1) to be the metastable ones. The conversion barrier (from **2** to **3**) was estimated to be about 12 kcal/mol using Car–Parrinello molecular dynamics simulations within the density functional theory framework. A tetra- $\sigma$ -bonded structure, **3**, has also been observed in a very recent STM experiment.<sup>21</sup>

In contrast, the most recent experiments performed by two different groups consistently predict the [4+2] product (**2**) to be the lowest energy species and the only reaction product for benzene on the Si(100) surface at saturation coverage and room temperature.<sup>22</sup> Witkowski and co-workers used polarization and angle-resolved NEXAFS techniques,<sup>22a</sup> and Shimomura and co-workers used photoelectron diffraction (PED) to draw the same conclusion.<sup>22b</sup> They both found *no evidence* for a more stable adsorption geometry. Possible surface conversion of **2** to tetra- $\sigma$ -bonded structures at longer time scales (that was proposed earlier) was not observed in both experiments at room temperature.

As shown in this brief review of the previous works, several issues regarding the adsorption of benzene on Si(100) are still not clearly understood, especially the configuration of the most stable product. The use of different experimental tools generated different results, and even similar STM techniques have been interpreted differently.<sup>15–18,21,23</sup> Various theoretical models have also been applied to this system, yet the questions still seem to remain unresolved. The current work presents a comprehensive *ab initio* study of the adsorption of benzene on Si(100). This includes the initial adsorption mechanisms, relative energetics of the products, and interconversion reactions among these products.

Following a summary of theoretical and computational methods in section II, results and discussion of them are presented in section III. Key concluding remarks are offered in section IV.

## II. Theoretical Methods

All calculations reported here were performed with the GAMESS (general atomic and molecular electronic structure system) electronic structure program.<sup>24</sup> A mixed basis set, consisting of the 6-31G(d) all-electron basis<sup>25</sup> for carbon and hydrogen atoms and the HW(d) effective core potential (ECP) basis<sup>26</sup> for silicon atoms, was used. We denote

this mixed basis as MIX. To assess the reliability of this mixed basis set, an all-electron basis set, DZV(d) consisting of the Dunning–Hay double- $\zeta$  valence basis plus d polarization functions, was also employed.<sup>27</sup> The Hessian matrix (matrix of energy second derivatives) was computed and diagonalized for all stationary points to characterize them. Intrinsic reaction coordinate (IRC) calculations, using the Gonzalez–Schlegel second-order method,<sup>28</sup> were conducted to verify that each saddle point connects the two minima of interest.

To describe benzene on Si(100) properly, the use of an adequate wave function is critical. Most of the adsorption products have at least one diradicaloid bare Si–Si dimer or conjugated (or just simple)  $\pi$  bond in which the gap between the bonding and the antibonding orbitals is close enough to allow configurational mixing. It is now well-established that the Si(100) bare surface can be correctly described only with multireference wave functions; this was first pointed out by Redondo and Goddard.<sup>29–34</sup> In addition, benzene loses its aromaticity during the adsorption process, and some of the delocalized  $\pi$  orbitals are converted to Si–C  $\sigma$  orbitals. Redistribution of this aromatic stabilization energy into newly formed  $\sigma$  bonds is best described by multireference wave functions. Therefore, since there are four active electrons and four dangling bonds in two silicon dimers and six active electrons and six delocalized  $\pi$  orbitals in the benzene molecule, CASSCF(10,10) wave functions (10 electrons in 10 orbitals complete active space SCF) are consistently used throughout the paper. To recover dynamic electron correlation, single-point energy calculations with the MRMP2 (multireference second-order perturbation theory) method<sup>35</sup> were performed at the CASSCF(10,10) optimized geometries. This is denoted by MRMP2//CASSCF(10,10).

A two-dimer Si<sub>31</sub>H<sub>28</sub> cluster was used to model the Si(100) surface because the benzene molecule is large enough to bridge across two dimers. However, Si<sub>31</sub>H<sub>28</sub>/C<sub>6</sub>H<sub>6</sub> is a rather large system for multireference perturbation theory methods. As an alternative, hybrid QM/MM (quantum mechanics/molecular mechanics) methods are becoming popular for modeling large molecular systems. In the QM/MM method, the chemically inactive region of the system is replaced by computationally inexpensive force field calculations, while the chemically active part, in which a reaction will occur, is still treated with full quantum mechanics. It has been shown that the SIMOMM (surface integrated molecular orbital molecular mechanics)<sup>36</sup> QM/MM method gives reasonable results at relatively low computational cost.<sup>31,33,34a</sup> In this work, the benzene molecule and the top two layers of the surface (10 silicon atoms in uppermost layers and corresponding terminating hydrogen atoms) are described by quantum mechanics, and the rest of the surface (21 bulk silicon atoms and corresponding terminating hydrogen atoms) by molecular mechanics (In Chart 1, the QM atoms are in blue and the MM atoms in gray.)

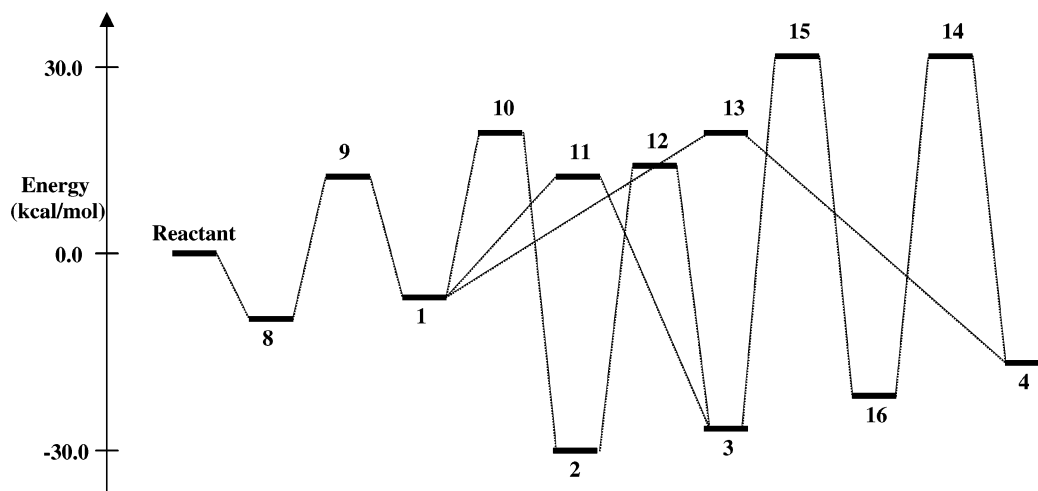
- (19) Kong, M. J.; Teplyakov, A. V.; Lyubovitsky, J. F.; Bent, S. F. *Surf. Sci.* **1998**, *411*, 286.  
 (20) Silvestrelli, P. L.; Ancilotto, F.; Toigo, F. *Phys. Rev. B* **2000**, *62*, 1596.  
 (21) (a) Naumkin, F. Y.; Polanyi, J. C.; Rogers, D.; Hofer, W.; Fisher, A. *Surf. Sci.* **2003**, *547*, 324–334. (b) Naumkin, F. Y.; Polanyi, J. C.; Rogers, D. *Surf. Sci.* **2003**, *547*, 335–348.  
 (22) (a) Witkowski, N.; Hennies, F.; Pietzsch, S.; Mattson, S.; Fohlish, A.; Wurth, W.; Nagasono, M.; Piancastelli, M. N. *Phys. Rev. B* **2003**, *68*, 115408. (b) Shimomura, M.; Munakata, M.; Honma, K.; Widstrand, S. M.; Johansson, L.; Abukawa, T.; Kono, S. *Surf. Rev. Lett.* **2003**, *10*, 499.  
 (23) Self, K. W.; Pelzel, R. I.; Owen, J. H. G.; Yan, C.; Widdra, W.; Weinberg, W. H. *J. Vac. Sci. Technol. A* **1998**, *16*, 1031.

- (24) Schmidt, M. W.; Baldrige, K. K.; Boatz, J. A.; Elbert, S. T.; Gordon, M. S.; Jensen, J. H.; Koseki, S.; Matsunaga, N.; Nguyen, K. A.; Su, S.; Windus, T. L.; Dupuis, M.; Montgomery, J. A., Jr. *J. Comput. Chem.* **1993**, *14*, 1347.  
 (25) (a) Hehre, W. J.; Ditchfield, R.; Pople, J. A. *J. Chem. Phys.* **1972**, *56*, 2257. (b) Francl, M. M.; Pietro, W. J.; Hehre, W. J.; Binkley, J. S.; Gordon, M. S.; Defrees, D. J.; Pople, J. A. *J. Chem. Phys.* **1982**, *77*, 3654.  
 (26) Hay, P. J.; Wadt, W. R. *J. Chem. Phys.* **1985**, *82*, 270.  
 (27) Dunning, T. H.; Hay, P. J. In *Methods of Electronic Structure Theory*; Schaefer, H. F., III, Ed.; Plenum Press: New York, 1977.  
 (28) Gonzalez, C.; Schegel, H. B. *J. Chem. Phys.* **1991**, *95*, 5853.  
 (29) Redondo, A.; Goddard, W. A., III. *J. Vac. Sci. Technol.* **1982**, *21*, 344.  
 (30) Paulus, B. *Surf. Sci.* **1997**, *375*, 55.  
 (31) Shoemaker, J.; Burggraf, J. W.; Gordon, M. S. *J. Chem. Phys.* **2000**, *112*, 2994.  
 (32) Gordon, M. S.; Shoemaker, J. R.; Burggraf, L. W. *J. Chem. Phys.* **2000**, *113*, 9355.  
 (33) Choi, C. H.; Gordon, M. S. *J. Am. Chem. Soc.* **1999**, *121*, 11311.  
 (34) (a) Jung, Y.; Choi, C. H.; Gordon, M. S. *J. Phys. Chem. B* **2001**, *105*, 4039. (b) Jung, Y.; Akinaga, Y.; Jordan, K. D.; Gordon, M. S. *Theor. Chem. Acc.* **2003**, *109*, 268–273.  
 (35) Nakano, H. *J. Chem. Phys.* **1993**, *99*, 7983.  
 (36) Shoemaker, J.; Burggraf, J. W.; Gordon, M. S. *J. Phys. Chem. A* **1999**, *103*, 3245.

**Table 1.** Relative Binding Energies (kcal/mol) of the Adsorption Products and Intermediates for the Reactions of Benzene on the Si(100) Surface

	reactant	1	2	3	4	5	8	16
This Work: SIMOMM (Si <sub>31</sub> H <sub>28</sub> /C <sub>6</sub> H <sub>6</sub> )								
CASSCF(10,10)/MIX <sup>a</sup>	0	0.4	-16.7	-10.4	0.1	42.7	2.1	-1.1
MRMP2//CASSCF(10,10)/MIX <sup>a</sup>	0	-3.9	-25.5	-24.4	-12.0	27.3	-7.4	-16.0
CASSCF(10,10)/DZV(d) <sup>b</sup>	0	0.3	-17.3	-8.5	-1.6		2.3	-1.7
MRMP2//CASSCF(10,10)/DZV(d) <sup>b</sup>	0	-6.3	-29.0	-26.7	-14.5		-8.9	-18.8
Previous Work								
Car-Parrinello MD/BLYP <sup>c</sup>	0	-17.8	-28.1	-35.3	-30.2			
DFT/B3LYP/6-31G(d)//HF/3-21G(d) <sup>d</sup>	0	-3.9	-20.2	-34.4	-21.0			

<sup>a</sup> Mixed basis set: HW(d) for Si and 6-31G(d) for H and C. <sup>b</sup> Geometries at the CASSCF(10,10)/MIX level were used. <sup>c</sup> Using a periodic slab model, ref 20b. <sup>d</sup> Using a Si<sub>15</sub>H<sub>16</sub> cluster model, ref 17.

**Chart 2**

### III. Results and Discussion

#### A. Adsorption Products and Their Relative Energetics.

Five potential candidates (1–5), suggested in the previous DFT and HF studies<sup>15–17</sup> as well as experiments as reaction products, were examined. The product configurations in which benzene links the two dimer rows have not been explored, since to our knowledge none of those products have been identified in experiments. However, it is noteworthy that other six-membered rings, such as 1,3-cyclohexadiene<sup>37</sup> and chlorinated benzene,<sup>21</sup> have been observed experimentally (with theoretical support) to add across dimer rows (over the dimer trench). Table 1 summarizes the relative energies of the products, and its schematic is shown in Chart 2. At the CASSCF(10,10) level of theory, only structures 2 and 3 are predicted to be bound (negative  $\Delta E$ ) relative to the reactants. However, with the MRMP2 single-point energy corrections at the same geometries, 1–4 are determined to be bound, while 5 is still unbound with respect to the reactants. This is consistent with the previous DFT//HF results.<sup>17</sup> Regardless of the adsorption products, qualitatively there are a few opposing forces affecting the stabilities (binding energies) of the products: the breaking of aromatic stability of benzene during adsorption, distortion of the surface, and some newly forming  $\sigma$  bonds between Si and C. Considering that all products except for 5 are bound at the MRMP2//CASSCF(10,10) level of theory, the formation of new Si–C  $\sigma$  bonds appears to be more important than the loss of aromaticity or surface distortion as a driving force for the

reaction. However, the creation of two radical centers in 5 upon adsorption makes this structure unstable relative to the reactants, even though 5 has four Si–C  $\sigma$  bonds. Because of this, 5 is not considered in the remainder of this paper.

Both CASSCF(10,10) and MRMP2//CASSCF(10,10) results consistently predict 2 to be the global minimum, although the preference for 2 relative to 3 is small when dynamic correlation is included. The di- $\sigma$ -bonded structures, 1 and 2, are similar to the [2+2] and [4+2] (i.e., Diels–Alder) cycloaddition products, respectively, even though both surface reactions involve breaking the aromaticity of benzene. It is well known that, in organic chemistry, [4+2] products are more stable than [2+2] products. This is not only because the [2+2] cycloaddition is a formally symmetry-forbidden reaction (kinetics), but also because the six-membered ring produced by the [4+2] cycloaddition has less ring strain than the four-membered ring produced by the [2+2] cycloaddition (thermodynamics). Therefore, it is reasonable that 2 is more stable than 1.

Isomers 3 and 4 are tetra- $\sigma$ -bonded structures. By forming two additional  $\sigma$  bonds relative to 1 and 2 and eliminating the Si–Si diradical bond, these structures might gain extra stabilization. However, to form these new  $\sigma$  bonds, the surface cannot avoid some degree of distortion. The interdimer Si–Si distances (i.e., Si1–Si3 and Si2–Si4 for 2 in Chart 1) for 1 and 2 are essentially the same as those in the bare cluster, as shown in Table 2. However, 3 and 4 have interdimer distances of 3.33 and 3.33 Å, and 3.35 and 3.68 Å, respectively, distorting the surface substantially compared to the bare surface (3.93 Å). So, this twisting of the surface (increasing the energy) and the

(37) Teague, L. C.; Boland, J. J. *J. Phys. Chem. B* **2003**, *107*, 3820–3823.

**Table 2.** Interdimer Surface Si–Si Distances (for **2**, for Example, These Correspond to Si1–Si3 and Si2–Si4 in Chart 1)

structure	Si1–Si3 (Å)	Si2–Si4 (Å)
bare surface	3.93	3.93
<b>1</b>	3.94	3.94
<b>2</b>	3.95	3.95
<b>3</b>	3.33	3.33
<b>4</b>	3.35	3.68
<b>5</b>	3.65	3.65
<b>7</b>	3.92	3.92
<b>8</b>	3.93	3.93
<b>9</b>	3.90	3.92
<b>10</b>	3.93	3.94
<b>11</b>	3.51	3.66
<b>12</b>	3.46	3.70
<b>13</b>	3.84	3.83
<b>14</b>	3.32	3.62
<b>15</b>	3.33	3.57
<b>16</b>	3.36	3.53

**Table 3.** CASSCF(10,10) Natural Orbital Occupation Numbers (NOON) for the Reaction Products (**1–5**) and Intermediates (**8** and **16**) in Chart 1, Corresponding to the Five Active Bonding Orbitals (Values in Parentheses Are Occupation Numbers for the Corresponding Antibonding Orbitals)

structure	NOON				
reactants	1.68 (0.32)	1.70 (0.30)	1.90 (0.10)	1.90 (0.10)	1.95 (0.05)
<b>1</b>	1.69 (0.31)	1.88 (0.12)	1.93 (0.07)	1.97 (0.03)	1.98 (0.02)
<b>2</b>	1.69 (0.31)	1.91 (0.09)	1.92 (0.08)	1.98 (0.02)	1.98 (0.02)
<b>3</b>	1.92 (0.08)	1.97 (0.03)	1.97 (0.03)	1.98 (0.02)	1.98 (0.02)
<b>4</b>	1.92 (0.08)	1.97 (0.03)	1.97 (0.03)	1.97 (0.03)	1.97 (0.03)
<b>5</b>	1.31 (0.69)	1.97 (0.03)	1.97 (0.03)	1.97 (0.03)	1.97 (0.03)
<b>8</b>	1.70 (0.30)	1.74 (0.26)	1.90 (0.10)	1.90 (0.10)	1.96 (0.04)
<b>16</b>	1.97 (0.03)	1.97 (0.03)	1.97 (0.03)	1.98 (0.02)	1.98 (0.02)

formation of additional  $\sigma$  bonds (decreasing the energy) are opposing forces in **3** and **4**. Comparison of MM energies (gray regions in Chart 1) also indicates that these surface distortions even cause the bulk (MM) energies in **3** and **4** to increase by 6–7 kcal/mol compared to the bare cluster.<sup>38</sup> Since **3** has a binding energy comparable to that of **2**, it is likely that these two factors cancel each other in **3**. Regarding the relative stability between **3** and **4**, it is difficult to rationalize their relative stabilities solely on the basis of such a simple structural argument, and it appears that more sophisticated electronic structure factors are involved.

To assess the reliability of the “mixed” basis set consisting of 6-31G(d) for carbon and hydrogen and HW(d) for silicon, all electron calculations with the DZV(d) basis were performed. As shown in Table 1, the two basis sets give very similar results, predicting **2** to be the global minimum and **3** to be very close to **2** in stability.

The results presented here disagree with previous (single-reference RHF, DFT, and semiempirical) calculations, in which **3** was predicted to be the lowest energy structure (Table 1). The previous calculations appear to overbind both **3** and **4**. This implies that the multireference character of the reactant and products **1** and **2** requires a more flexible wave function.

The CASSCF(10,10) natural orbital occupation numbers (NOON) for the reaction products (and intermediates) are listed in Table 3. (The complete list of NOONs for all stationary points is provided in Supporting Information.) Large occupation numbers for the active antibonding orbitals of **1** and **2** illustrate

(38) Energies of the MM region (calculated using MM3 parameters) for the reactants and **1–4** are  $-4.5$ ,  $-4.8$ ,  $-5.9$ ,  $+2.0$ , and  $+1.1$  kcal/mol, respectively.

that the multireference character of these structures, as well as that of the reactants, is much greater than those of **3** and **4**. Indeed, **3** and **4** appear to be essentially single reference species. Consequently, the single reference methods will tend to underestimate the relative stabilities of **1** and **2**. Therefore, multireference wave functions are necessary in order to consistently describe the potential energy surface of benzene on the Si(100) surface. However, since **2** and **3** are predicted to differ by only a few kilocalories per mole, the relative energies of these two species could change if one examined the potential energy surface with MRMP2 geometries and increased the size of the basis set. Also, due to the different number of Si–C  $\sigma$  bonds (for which a sufficient amount of dynamic correlation is required for quantitative analysis) in different reaction products (e.g., di- $\sigma$  versus tetra- $\sigma$ ), it is possible that including more dynamic correlation than is present in MRMP2 could change the relative energetics.

Chart 1 also shows selected geometric parameters. The surface silicon atoms forming dimers rehybridize when they form new  $\sigma$  bonds with the carbon atoms. In other words, partial  $\pi$  bonds arising from the dangling bonds of the bare surface dimer are essentially destroyed when they form  $\sigma$  bonds. The surface Si–Si bonds then become bulklike  $sp^3$ -hybridized Si–Si single bonds with bond lengths of  $\sim 2.34$  Å. The actual rehybridized Si–Si dimer bond length varies a bit, ranging from 2.31 to 2.35 Å, for different reaction products, because the degree of the ring strain forced by benzene for different products varies also. For **1** and **2**, the dimers that are not directly involved in the surface reaction remain intact with dimer bond lengths of 2.24 Å, the same as that of a bare dimer. For comparison, the clean surface dimer has a bond length of 2.24–2.28 Å, depending upon the cluster size used at the CASSCF level, and 2.24 Å according to experiment.<sup>31,39</sup>

The structure of benzene also changes significantly upon adsorption. Due to the loss of aromaticity upon surface reaction, the C–C bond of benzene (1.40 Å) with a formal bond order of 1.5 changes to either a single (1.51–1.59 Å) or a double (1.34 Å) bond as a result of the reaction. The modified single bond in benzene varies (somewhat significantly) for different reaction products (1.51–1.59 Å) due to the varying strain forced by the topology of the surface. The newly formed C–Si covalent  $\sigma$  bond also varies (but only slightly) from 1.95 to 1.98 Å.

**B. Initial Adsorption Mechanisms (Di- $\sigma$ -Bonded Structures, **1** and **2**). [4+2] Cycloaddition Mechanism.** Structure **2** is a symmetry-allowed [4+2]-like cycloaddition adduct, and thus one would expect a small or zero reaction barrier for the formation of **2** from the reactants. However, the CASSCF(10,-10) barrier is calculated to be 17.7 kcal/mol. The stationary point **7** (See Chart 1) yielding this barrier height is a true transition state, as characterized by the CASSCF(10,10) Hessian followed by the IRC. However, subsequent MRMP2 single-point energy calculations on the reactant, **7**, and **2** lead to the prediction that **7** has a lower energy than the reactant. This could mean either that there is really no barrier (and that structure **7** is not a stationary point) at the higher level of theory, or that the MRMP2 transition state geometry is very different from that predicted by CASSCF(10,10). To shed some light on this, a series of MRMP2 single-point calculations were performed along the CASSCF(10,10) IRC. The results are presented in

(39) Wang, Y.; Shi, M.; Rabalais, J. W. *Phys. Rev. B* **1993**, *48*, 1689.



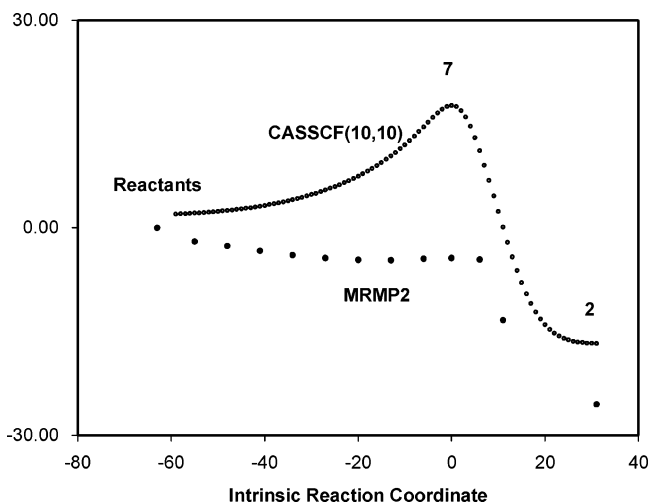


**Figure 1.** CASSCF(10,10)/MIX potential energy curves (○) along the intrinsic reaction coordinate of the [4+2] cycloaddition reaction (from reactants to **2** via **7**). After refinement with MRMP2 correction (●), the barrier disappears, as is usual [4+2] addition reactions.

Figure 1. The MRMP2 energies decrease almost monotonically as the geometry changes along the CASSCF(10,10) minimum energy path from the reactant to **2**. Therefore, while the complete MRMP2 potential energy surface is not currently obtainable, the MRMP2//CASSCF(10,10) level of theory suggests that the [4+2] addition of benzene to the Si(100) surface occurs with little or no barrier. This result is in accord with the usual [4+2] cycloaddition energetics (a small or zero reaction barrier). That a 17.7 kcal/mol of CASSCF(10,10) reaction barrier essentially disappears at the MRMP2//CASSCF(10,10) level of theory clearly suggests that dynamic electron correlation is very important for this system.

Finally, note that the prediction that the [4+2] reaction of benzene on Si(100) is barrierless is in disagreement with a recent paper by Alavi and co-workers.<sup>40</sup> On the basis of B3LYP cluster calculations, the authors predicted the [4+2] adsorption of benzene to occur via an intermediate (physisorbed configuration) and a single transition state. In their study, the activation barrier was estimated to be about 4 kcal/mol.

**[2+2] Cycloaddition Mechanism.** The [2+2] cycloaddition is symmetry-forbidden according to the Woodward–Hoffmann rules. However, it has been shown that the [2+2] reaction for 1,3-cyclohexadiene on the Si(100) surface can also occur with ease (i.e., activation energy of about 4–8 kcal/mol) if the reaction follows a nonsymmetric pathway.<sup>33</sup>

Since it was not possible to locate transition state(s) for this mechanism at the CASSCF(10,10) level despite an extensive search, spin-polarized DFT with the B3LYP functional (denoted UB3LYP) was used.<sup>41,42</sup> UB3LYP has been demonstrated to be capable of yielding reasonable structures for the Si(100)

**Table 4.** Relative Energies (in kcal/mol) of the Structures along the [2+2] Mechanism Forming **1**

	reactants	<b>8</b>	<b>9</b>	<b>1</b>
UB3LYP/MIX	0	−1.9	11.5	−10.5
CASSCF(10,10)/MID <sup>a</sup>	0	2.1	22.9	−0.3
MRMP2/MIX <sup>a</sup>	0	−7.4	12.3	−7.1
CASSCF(10,10)/DZV(d) <sup>a</sup>	0	2.3	22.0	−0.2
MRMP2/DZV(d) <sup>a</sup>	0	−8.9	8.9	−9.8

<sup>a</sup> Geometries at the UB3LYP/MIXED level were used.

surface.<sup>43</sup> The energetics of the UB3LYP transition structures were then refined using the multireference and MRMP2 wave function methods, as summarized in Table 4. A schematic for this mechanism can also be seen in Chart 2.

One weakly bound complex (**8**) and one transition state (**9**) were found using UB3LYP/MIX, with partial structures shown in Chart 1. The structural characteristics of **8** (namely, the long C2–Si2 (3.27 Å) and C1–Si1 (4.36 Å) distances, and the intact Si–Si dimer and benzene) suggest that it indeed corresponds to a weakly bound van der Waals (VDW) complex. This intermediate is 1.9 kcal/mol lower in energy than the reactants at the UB3LYP level. However, single-point MRMP2(10,10)/MIX calculations (which include both strong nondynamic and dynamic correlation effects) find this VDW complex (**8**) to be comparatively strongly bound (−7 to −9 kcal/mol) relative to the reactants. The stability of **8** is in fact comparable to that of the [2+2] product (**1**).

The MRMP2/DZV(d) reaction barrier for **8** to become the final product (**1**) is 17.8 kcal/mol. This barrier is somewhat large compared to the analogous nonsymmetric one-step [2+2] reaction of 1,3-cyclohexadiene on Si(100) (4–8 kcal/mol).<sup>33</sup> This difference probably arises due to the fact that the reaction of **8** to form **1** breaks the aromaticity of benzene. However, the net barrier from separated reactants to **1** is only 8.9 kcal/mol. This is the most relevant barrier except at very low temperatures. Note also that, although there have been some theoretical proposals that similar [2+2] reactions of 1,3-cyclohexadiene<sup>37</sup> on Si(100), ethylene<sup>44a</sup> on Si(100), and butadiene<sup>44b</sup> on Si(100) might occur via a two-step diradical or zwitterionic mechanism, no such intermediates have been found for the [2+2] reaction of benzene with Si(100), and hence no such nonconcerted channel has been identified.

Finally, note that single-point CASSCF(10,10) energy calculations predict **8** to be unbound with respect to the reactants. The MRMP2 correction stabilizes **8** and makes it bound. This shows the importance of including dynamic correlation (which is the main quantum mechanical origin of dispersion attractions) to describe the VDW complex. The MRMP2 basis set effects are small (Table 4), except that the barrier is ~3 kcal/mol smaller when the all-electron basis set is used.

**C. Surface Conversion Reactions and the Formation of Tetra-σ-Bonded Products (3 and 4).** As mentioned in the Introduction, some experimental reports in the literature have emphasized the possibility that the adsorption products can dynamically isomerize and interconvert to different configurations as a function of time. Therefore, in this work all possible interconversion reactions among the reaction products, **1–4**,

(40) Alavi, S.; Rousseau, R.; Seideman, T. *J. Chem. Phys.* **2000**, *113*, 4412.

(41) At the CASSCF(10,10) level, careful efforts to find a TS for the [2+2] mechanism (TS<sub>[2+2]</sub>) yielded only a transition structure that actually connects the [2+2] and the [4+2] products, namely, **10** in Chart 1. This suggests that, at least at this level of theory, TS<sub>[2+2]</sub> is very similar to **10**. Indeed, the TS<sub>[2+2]</sub> found at the UB3LYP level (structure **9** in Chart 1) is similar to **10** (a transition structure for the [2+2]-to-[4+2] isomerization at CASSCF(10,10)). Note that we also tried to find a TS<sub>[2+2]</sub> at the CASSCF(10,10) level starting from **9**, but again we obtained only **10**.

(42) There have been some recent indications that B3LYP overestimates the degree of delocalization for aromatic (annulenes,  $n > 6$ ) systems [Wannere, C. S.; Schleyer, P. v. R. **2003**, *5*, 865–868]. However, benzene is small enough that it should be described properly by DFT.

(43) Jung, Y.; Yiham, S.; Gordon, M. S.; Doren, D.; Head-Gordon, M. *J. Chem. Phys.* **2003**, *119*, 10917.

(44) (a) Lu, X. *J. Am. Chem. Soc.* **2003**, *125*, 6384–6385. (b) Minary, P.; Tuckerman, M. E. *J. Am. Chem. Soc.* **2003**, *126*, 13920–13921.

**Table 5.** Activation Barriers (in kcal/mol) for the Surface Conversion Reactions among the Adsorption Products (See Also Chart 2)

	10 (from 1 to 2)	11 (from 1 to 3)	12 (from 2 to 3)	13 (from 1 to 4)	14 (from 4 to 16)	15 (from 16 to 3)
CASSCF(10,10)/MIXED	48.5	30.5	74.4	35.0	57.6	58.8
MRMP2//CASSCF(10,10)/MIXED	19.9	11.3	38.5	24.6	41.3	47.1
CASSCF(10,10)/DZV(d)	22.5	31.1	46.7	33.8	55.7	61.0
MRMP2//CASSCF(10,10)/DZV(d)	19.1	15.5	37.0	21.4	37.9	45.4

have been systematically examined. Energy barriers associated with these isomerization reactions are tabulated in Table 5, and a schematic of the competing processes is presented in Chart 2.

#### Isomerization between [2+2] (1) and [4+2] (2) Products.

The transition state for this isomerization is depicted as **10** in Chart 1. The MRMP2/DZV(d)//CASSCF(10,10)/MIXED reaction barrier for the 1-to-2 conversion is 19.1 kcal/mol. The 2-to-1 reverse reaction involves a huge (41.8 kcal/mol) activation barrier, as is evident from the fact that **2** is energetically much more stable than **1**. The reverse barrier is larger than the ~23 kcal/mol barrier predicted by Borovsky et al.<sup>18</sup> on the basis of an Arrhenius prefactor of  $10^{13}$  Hz, their STM experiments, and the PM3 calculations of Jeong et al.<sup>12</sup>

Although the 1–2 conversion (19.1 kcal/mol) of benzene on Si(100) is easier than the 2–1 reverse isomerization (41.8 kcal/mol), and is also much easier than the same (1–2) reaction (42.2 kcal/mol) for 1,3-cyclohexadiene adsorbed on Si(100), it still requires a relatively large activation barrier (19.1 kcal/mol) for **1** to isomerize into **2**. This means that, once formed, **1** and **2** are unlikely to interconvert with ease (at least at moderate temperatures), even though **2** (the [4+2] product) is more stable than **1** (the [2+2] product). So, for temperatures at which **1** is accessible, it is likely to be observed as a product.

The bond length of 2.35 Å for the reacting silicon dimer (**10** in Chart 1) indicates that this moiety has lost its diradical (and partial  $\pi$  bonding) character and has already rehybridized at the transition state. This is consistent with the NOONs that are very closed-shell-like (see Supporting Information).

**The Formation of 3.** Tetra- $\sigma$ -bonded product **3** can be obtained most easily from di- $\sigma$ -bonded products **1** and **2** by forming two additional  $\sigma$  bonds with an adjacent dimer in the same row. The formation of **3** from **2** is similar to the [2+2] reaction discussed above, since the C2=C3 double bond in **2** is reacting with a Si–Si dimer that is also a partial double bond. The MRMP2/DZV(d)//CASSCF(10,10) energy barrier for the isomerization from **2** to **3** is predicted to be 37.0 kcal/mol via transition state **12**, suggesting that **2** is kinetically stable with respect to the conversion to **3**. This is in sharp contrast to the previous predictions, based on single reference and semiempirical methods, that **2** is metastable and the 2–3 conversion involves only a 12–22 kcal/mol activation barrier.<sup>15,20</sup>

Although this reaction pathway from **2** to **3** is not symmetric (2.43 and 3.11 Å for C2–Si1 and C3–Si2 lengths, respectively, in **12**), both C2 and C3 form their new bonds in a concerted manner. So, although the process is not strictly Woodward–Hoffmann forbidden, this concerted reaction path (plus some distortion of the surface and benzene) results in a substantial reaction barrier (37.0 kcal/mol) that resembles a [2+2] process.

On the other hand, the formation of **3** from **1** is formally a [4+2] reaction since the carbon chain (C1=C2–C3=C4 in **1**) in benzene participating in this conversion reaction is similar

to 1,3-butadiene reacting with Si–Si dimer dangling bonds (or a partial double bond). Unlike the usual barrierless [4+2] reaction, however, it does involve the transition state (**11**), shown in Chart 1 with a corresponding MRMP2/DZV(d)//CASSCF(10,10) barrier of 15.5 kcal/mol. This is a significant barrier for this type of reaction. The transition-state geometry (**11**) suggests that this reaction occurs in a nonsymmetric manner, unlike the usual symmetric [4+2] reaction. At this TS, C1–Si1 is 3.40 Å whereas C4–Si2 is 2.48 Å. Inspection of the detailed transition-state geometry reveals that it involves a structural distortion not only of the surface but also of benzene (Chart 1 and Table 2). This may be the origin of the barrier. However, the barrier from **1** to **3** is still much smaller than that for the 2–3 mechanism (37.0 kcal/mol), which is “formally” a [2+2] reaction. Therefore, it is suggested that **3** is formed kinetically mostly via **1** if the accessible thermal energy is greater than 15 kcal/mol. Moreover, as will be discussed later, the formation of **3** via **4** involves an even higher barrier. This supports the conclusion that **3** is formed primarily from **1**.

**The Formation of 4.** **4** is another tetra- $\sigma$ -bonded product to which **1** can isomerize, by forming two additional  $\sigma$  bonds without breaking any existing  $\sigma$  bonds. The conversion of **1** to **4** is also a [2+2]-type reaction in which the C1=C2 double bond reacts with the Si1–Si2 partial double bond. The two  $\sigma$  bonds are created in a single step in this reaction (concerted), but the transition structure (**13**) is not symmetric: the newly forming carbon–silicon  $\sigma$  bond lengths are 3.32 and 2.36 Å. This is very similar to the [2+2] mechanism for the 2–3 conversion (through **12**) described above, except that this 1–4 isomerization (through **13**) has a much smaller barrier (21.4 kcal/mol) than the 2–3 isomerization (37.0 kcal/mol) at the same level of theory. The difference apparently arises mainly from the difference in the degree of surface distortion in the two transition structures. While they both include some degree of surface distortion (i.e., interdimer Si–Si distances are 3.70 and 3.46 Å for **12**, 3.84 and 3.83 Å for **13**, and 3.93 and 3.93 Å for the bare dimers in Table 2), it is clear that **12** (the transition state that connects **2** and **3**) is structurally more twisted than **13** (the transition state that connects **1** and **4**).

One might also consider the formation of **4** from the di- $\sigma$ -bonded product, **2**. However, this involves breaking the C4–Si4 bond in **2** and rotating benzene about 90° to create three new  $\sigma$  bonds. Although attempts to find a simple one-step reaction pathway for this isomerization were not successful, the process can occur via two steps: isomerization from **2** to **1**, followed by isomerization from **1** to **4**. The net reaction barrier for this two-step process would be the same as that for the 2–1 isomerization reaction.

**Isomerization between 3 and 4.** Next, consider the isomerization between the two tetra- $\sigma$ -bonded products, **3** and **4**. This process is predicted to occur through an intermediate, **16**, which is another tetra- $\sigma$ -bonded minimum (Chart 1). This intermediate

has a binding energy comparable to and slightly lower than that of **4** (Table 1). At a first glance, **16** looks similar to the unstable product **5** with two diradical sites. However, unlike **5**, **16** has an additional covalent bond that is formed between the two carbon radical sites, thereby stabilizing the structure. This bicyclic compound also has two newly formed Si–C  $\sigma$  bonds. The stability of this conformation can also be deduced from the NOONs in Table 3: due to its valence-saturated nature, **16** is essentially a closed-shell molecule.

The isomerization between **3** and **4** through intermediate **16** involves substantial barriers. The isomerization from **4** to **16** traverses a barrier of 37.9 kcal/mol at **14**, and the second transition state (**15**) connecting this intermediate (**16**) with **3** has a barrier of 45.4 kcal/mol. This suggests that, although **16** is thermodynamically quite a stable species (about 10 kcal/mol above the global minimum, (**2**), the reaction to form **16** is kinetically unlikely.

#### IV. Conclusions

A comprehensive ab initio study of the adsorption of benzene on the Si(100) surface predicts that structure **2** (the [4+2]-like product) is the most stable configuration. High activation barriers ( $\sim 40$  kcal/mol) for the conversion of **2** to form other products suggest that **2** is stable kinetically as well as thermodynamically. This is consistent with recent experiments,<sup>22</sup> but inconsistent with previous theoretical predictions based on single reference methods (restricted Hartree–Fock, density functional theory, and semiempirical) in which **2** was predicted to be metastable and to convert to **3** with 12–22 kcal/mol activation barriers.<sup>15,20</sup> Together with the significant CASSCF(10,10) natural orbital occupation numbers for several stationary points on the potential energy surface, this suggests that a wave function with sufficient flexibility to account for multireference character is necessary for a correct description of reactions of benzene on Si(100).

The degree of surface distortion and the number of newly formed Si–C  $\sigma$  bonds are the two main opposing factors determining the stabilities (binding energies) of the products. Isomers **2** (two new Si–C  $\sigma$  bonds and minor surface strain) and **3** (four new Si–C  $\sigma$  bonds and substantial surface strain) are predicted to have the largest binding energies. Isomer **5** is predicted to be unbound relative to the reactant because it has two radical centers.

At the highest level of theory used in this study (MRMP2/DZV(d)//CASSCF(10,10)/MIX), the [4+2] cycloaddition of benzene on the Si(100) surface is found to be barrierless, even though the reaction involves the loss of benzene aromaticity. Comparison of MRMP2 single points on the potential energy surface with CASSCF(10,10) energies for the [4+2] cycloaddition mechanism illustrates that dynamic electron correlation is important for this system.

The asymmetric [2+2] addition of benzene on Si(100) occurs with a net reaction barrier of 8.9 kcal/mol. The initial step for this mechanism is predicted to be the formation of a VDW complex intermediate, which is 8.9 kcal/mol more stable than the reactants. The relatively high activation barrier of 17.8 kcal/mol relative to the VDW intermediate, compared to that for the similar [2+2] reaction of 1,3-cyclohexadiene on Si(100)

(4–8 kcal/mol), is probably due to the fact that the cycloaddition reaction of benzene from the VDW structure involves the breaking of its aromaticity. Nonetheless, the net barrier relative to reactants is only slightly larger than that reported previously for cyclohexadiene.

Surface isomerizations were also considered. Two tetra- $\sigma$ -bonded products, **3** and **4**, can be most easily formed by conversion of the [2+2] product as long as sufficient thermal energy is available to overcome the barriers, 15.5 and 21.4 kcal/mol for the **1–3** and **1–4** conversions, respectively. Isomerizations from **2** to **3** or **4** must overcome very large activation barriers. This suggests that **1** must be the precursor for **3** or **4** observed in experiments. This means that at least about 20 kcal/mol of thermal energy (needed to overcome the [2+2] transition state) is required to have tetra- $\sigma$ -bonded products in experiments. The [2+2]-to-[4+2] (**1–2**) isomerization requires a similar 19.1 kcal/mol activation energy.

Of course, the two-dimer cluster model employed in this study may not be sufficient to describe all possible reactions of benzene on Si(100). For example, a previous study suggested that some surface properties are not converged at the two-dimer cluster.<sup>42</sup> In this sense, one would like to use a slab approach for a more realistic representation of the surface, since a slab is free of edge effects. However, as shown above, DFT, with which the slab approach is usually implemented, is not appropriate for diradicaloid systems such as Si(100). Hence, ideally one would like to do slab calculations with MRMP2. In practice, this is not currently feasible, so one has to rely on finite cluster models in order to use multireference wave functions. This finite cluster approach can then be improved by using an embedded cluster method such as the SIMOMM method employed here.

Finally, the low-temperature IR and NEXAFS experiments performed by Kong et al. suggested that the physisorbed configuration of benzene on Si(100) was dominant at 100 K. This physisorbed product most likely corresponds to the VDW complex, **8**. The [4+2] product (predicted here to be barrierless) was not detected in their experiments. This could mean that MRMP2 geometries are sufficiently different from the CASSCF-(10,10) geometries that there is indeed some reaction barrier for the [4+2] mechanism (as found in ref 36), that higher levels of theory or larger basis sets are required, or that the chemisorbed product does exist on the surface. To confirm the predicted activation barriers presented here, improved calculations at higher levels of theory and a systematic experimental study at various temperatures are both desirable.

**Acknowledgment.** This work was supported by a grant from the Air Force Office of Scientific Research. The calculations were performed on an Alpha Cluster, obtained by grants from the Department of Energy and the National Science Foundation.

**Supporting Information Available:** Optimized geometries for all stationary points found in this work and CASSCF active natural orbital occupation numbers at those structures. This material is available free of charge via the Internet at <http://pubs.acs.org>.

JA0402093